

Mei Ni Yuan*, Yan Qing Yang, Qiao Juan Gong, Chao Li and Xian Zhong Lang

Microstructure-based modeling of the dynamic mechanical properties of SiCp/Al composites

Abstract: Using image processing and recognition, a microstructure-based finite element model (FEM) was established to predict the dynamic properties of SiCp/Al composites at different strain rates ranging from 200 to 14,000 s⁻¹. In the microstructure-based FEM, the irregular SiC particles were randomly distributed in the matrix, and its configurations did not change. The results showed that the flow stress of SiCp/Al composites with low particle volume fraction first increases and then decreases with the increasing of strain rate during the adiabatic compression. The reducing flow stress of SiCp/Al composites is caused by the inner damage and the heat softening of composites. The angular particles in SiCp/Al composites provide more strengthening effect than the circle particles when the strain is <0.62, while the circle particles provide more strengthening effect than the angular particles for strain >0.62.

Keywords: dynamic mechanical analysis; metallic composites; microstructure; simulation and modeling.

DOI 10.1515/secm-2013-0223

Received September 25, 2013; accepted July 8, 2014; previously published online January 13, 2015

1 Introduction

Particle-reinforced metal matrix composites (PRMMC) are widely used in aerospace, aviation, and arms structural components, owing to their high specific strength, high thermal conductivity, excellent abrasion resistance, and other properties. In the aerospace, aviation, and arms

*Corresponding author: Mei Ni Yuan, College of Mechanical and Electrical Engineering, North University of China, Taiyuan 030051, P.R. China; and The State Key Laboratory of Solidification Processing in Northwestern Polytechnical University, Xi'an 710072, P.R. China, e-mail: mnyuan@126.com

Yan Qing Yang: The State Key Laboratory of Solidification Processing in Northwestern Polytechnical University, Xi'an 710072, P.R. China

Qiao Juan Gong: Department of Applied Chemistry, Yuncheng University, Yuncheng Shanxi 044000, P.R. China

Chao Li and Xian Zhong Lang: College of Mechanical and Electrical Engineering, North University of China, Taiyuan 030051, P.R. China

application fields, PRMMC inevitably suffer the high-speed crash and impact of bullets, birds, space dust, etc. Thus, the dynamic mechanical properties of PRMMC should be comprehensively understood. Zhang et al. [1] analyzed the dynamic behaviors of Al₂O₃/6061-T6Al composites using the multiparticle two-dimensional (2D) finite element model (FEM). Chen and Ghosh [2] established a unit cell model to investigate the deformation and damage in SiC/Al7075-T6 composites. Lim and Dunne [3] studied the dynamic mechanical properties of SiC/Al composites using the unit cell approach. Zhang et al. [4] built an axisymmetric unit cell model to investigate the dynamic mechanical behaviors of PRMMC. In their simulations, the particle shapes were assumed as idealized sphere or ellipsoid. Additionally, some experiments were conducted to characterize the dynamic behaviors of PRMMC [5–7].

In this article, with the use of image processing, geometric modeling, and finite element meshing, a 2D microstructure-based FEM was built to investigate the dynamic mechanical properties of SiCp/Al composites.

2 Finite element modeling

2.1 Finite element model

The scanning electron microscopic (SEM) photograph of SiCp/Al composites, which is shown in Figure 1A, was converted to vector format using image processing and recognition [8]. Then, on the basis of the vector image, a computer-aided drafting (CAD) model, shown in Figure 1B, was developed using computer-aided design software. Finally, the developed CAD model was imported into ABAQUS software and meshed, and the 2D microstructure-based FEM was obtained, as shown in Figure 1C. The boundary conditions imposed on the microstructure-based FEM are shown in Figure 1C.

The dynamic compressive load was simulated by imposing displacement $U_y(x, b)$ on all the nodes in $y=b$, given as Formula (1). The node displacements at $y=0$ in Y direction were assumed to be zero, as in Formula (2).

$$U_y(x, b) = u \times \text{Amp}, \quad (1)$$

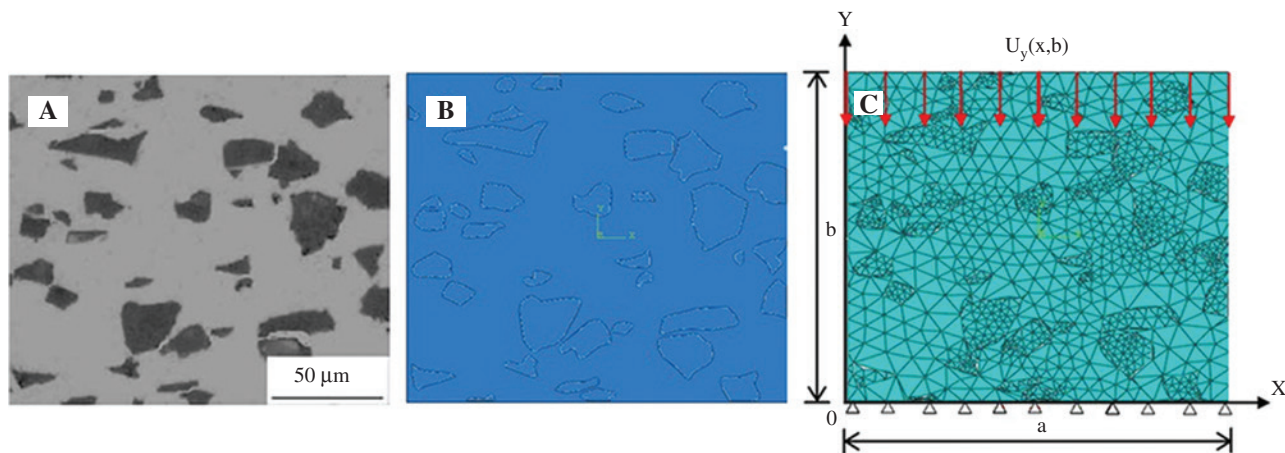


Figure 1 Stages of conversion of SEM image into FEM.
(A) SEM image; (B) CAD model; and (C) FEM.

$$U_y(x,0)=0, \quad (2)$$

where u is the displacement and Amp is the displacement as a function of times.

2.2 Material model

Al alloy was modeled using the Johnson-Cook model. The flow stress in the Johnson-Cook model is expressed as

$$\sigma = [a + b\epsilon^n][1 + e \ln \epsilon^*][1 - T^{*m}] \quad (3)$$

$$T^* = \frac{(T-298)}{(T_{\text{melt}}-298)} \quad (4)$$

where σ , ϵ , ϵ^* , and n are the dynamic flow stress, plastic strain, plastic strain rate, and work hardening exponent, respectively; a , b , e , and m are all constant; and T_{melt} is the melting temperature.

In addition, the JH-2 model is used to characterize the SiC particle. The flow stress in the JH-2 model is expressed as

$$\sigma = \frac{[\sigma_i^* \cdot D(\sigma_i^* - \sigma_f^*)]}{\sigma_{\text{HEL}}}, \quad (5)$$

where σ_i^* , σ_f^* , σ_{HEL} , and D are the normalized intact equivalent stress, the normalized fractured equivalent stress, the equivalent stress at the Hugoniot elastic limit (HEL), and the damage variable, respectively. σ_i^* and σ_f^* can be expressed as

$$\sigma_i^* = A \left(\frac{P}{P_{\text{HEL}}} + \frac{T}{P_{\text{HEL}}} \right)^N (1 + C \ln \epsilon^*), \quad (6)$$

$$\sigma_f^* = B \left(\frac{P}{P_{\text{HEL}}} \right)^M (1 + C \ln \epsilon^*), \quad (7)$$

where A , B , C , M , and N are all constants; P , P_{HEL} , T , and ϵ^* are the actual pressure, the pressure at the HEL, the maximum tensile pressure, and the plastic strain rate, respectively. The material parameters of Al and SiC are listed in Table 1.

3 Results and discussion

3.1 Effect of strain rate

The predicted dynamic compressive stress-strain curves of SiCp/Al composites are shown in Figure 2. The SiC particle

Table 1 Material parameters of Al and SiC.

Al	ρ (kg m ⁻³)	c [J (kg K) ⁻¹]	T_{melt} (K)	a	b	n	e	m
	2702	880	660	369	684	0.73	0.0083	1.7
SiC	A	B	C	N	M	$K1$	$K2$	$K3$
	0.96	0.35	0.009	0.65	1.0	220	361	0
	$D1$	$D2$	ρ	σ_i^{max}	Shear modulus	σ_f^{max}	$\epsilon_{f\text{max}}$	$\epsilon_{f\text{min}}$
	0.48	0.48	3215	12.2	193	1.3	1.2	1.0
	HEL	P_{HEL}	T	Poisson ratio	Beta	IDamage	Fs	
	11.7	5.13	0.75	0.3	1.0	0	0.2	

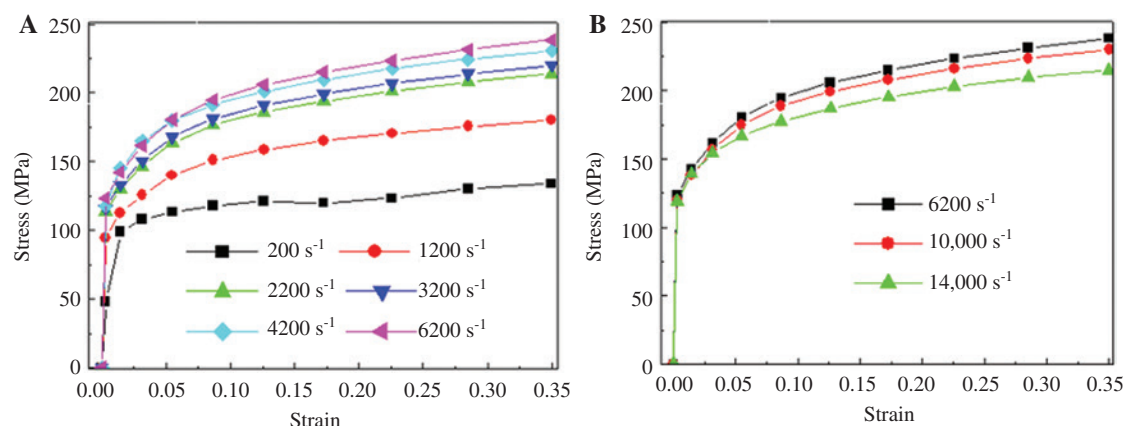


Figure 2 Stress-strain behaviors of SiCp/Al composites at different strain rates.

volume fraction was 0.15. From Figure 2A, it can be seen that the flow stresses of SiCp/Al composite increase with increasing strain rate ranging from 200 to 6200 s⁻¹. The increasing tendency becomes small when the strain rate exceeds 3200 s⁻¹. This observation is consistent with the experimental results reported by Perng et al. [8].

However, when the strain rate exceeds 6200 s⁻¹, the flow stresses of SiCp/Al composites decrease with increasing strain rate, as shown in Figure 2B. Inner damage and matrix heat softening in SiCp/Al composites were observed during the adiabatic compression. This decreasing tendency is caused by the inner damage and the heat softening of composites. The SEM photographs of SiCp/Al composites can show the locally melting phenomenon of the matrix [6]. Zhu et al. [9] also found that there were some cavities, microcracks, particle fracture, and matrix softening performance in SiCp/2024Al composites by using SEM. Leduc and Bao [10] and Zhou and Xia [11] also found that thermal softening has an obvious influence on the flow stress in PRMMC.

3.2 Effect of particle shape

Dynamic compression simulations of SiCp/Al composite with different particle shapes were conducted, as shown in Figure 3. The results indicated that when the strain is <0.62, the original, square, and hexagon particles (i.e., angular particle) provide more stress and strengthening effect than the circle particle. The reason is that the constraint of the angular particle is high. The high constraint of the angular particle results in the high local stress concentration phenomenon, and is more beneficial in causing matrix hardening.

In contrast, the circle particle provides more stress and strengthening for strain (>0.62). The reason is that when the strain is >0.62, most angular particles are fractured because the local stress is higher than the fracture stress of the angular particle. The higher local stress results from the stress concentration phenomenon. However, the circle particles result in the low local stress concentration phenomenon and local stress. Thus, a few circle particles failed. Song et al. [12] also found that the angular particle fractures more easily than the circle particle.

3.3 Effect of particle volume fraction

Dynamic compression simulations of SiCp/Al composites with different SiC particle volume fractions were conducted, as shown in Figure 4. It can be clearly seen that the elastic modulus of SiCp/Al composites increases with increasing SiC particle volume fractions. Meanwhile, the flow stress-strain curve of SiCp/Al composites increase

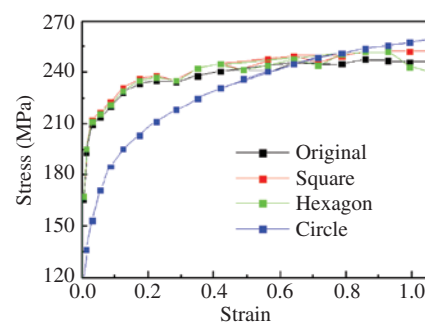


Figure 3 Stress-strain behaviors of SiCp/Al composites with different particle shapes.

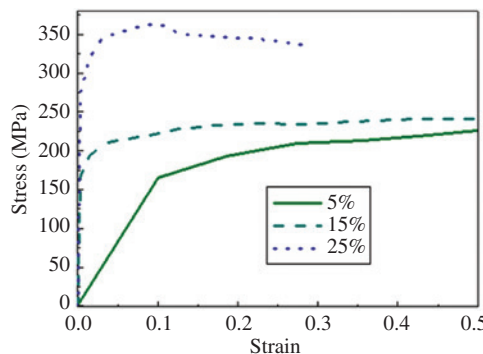


Figure 4 Stress-strain behaviors of SiCp/Al composites with different SiC particle volume fractions.

with increasing SiC particle volume fractions. The reason is that the higher the SiC particle volume fraction is, the more the grain refinement and dislocations interaction in matrix are, which results in higher flow stress in PRMMC. According to the Orowan dislocation theory, the curvature radius of dislocation increases with increasing particle volume fraction, which leads to a higher flow stress.

4 Conclusions

A microstructure-based FEM was constructed to investigate the dynamic mechanical properties of SiCp/Al composites. The results showed that (i) the flow stress of SiCp/Al composites first increases and then decreases with increasing strain rate. (ii) When the strain is <0.62 , the angular particle provides more stress and strengthening

effect than the circle particle. However, the circle particle provides more strengthening for the strain (>0.62). (iii) The flow stress and elastic modulus increase with increasing particle volume fractions.

Acknowledgments: The authors acknowledge the financial support provided by the Natural Science of China (51201155), the Natural Science of Shanxi province (2012011019-1, 2012011007-1), and the Chinese Education Ministry Foundation for Doctors (20101420120006).

References

- [1] Zhang JT, Liu LSh, Zhai PC. *Compos. Sci. Technol.* 2007, 67, 2775–2785.
- [2] Chen YL, Ghosh S. *Int. J. Plasticity* 2012, 32, 218–247.
- [3] Lim LG, Dunne FPE. *J. Mech. Sci.* 1996, 38, 19–39.
- [4] Zhang H, Ramesh KT, Chin ESC. *Acta Mater.* 2005, 53, 4687–4700.
- [5] Hayun S, Dariel MP, Frage N, Zaretsky E. *Acta Mater.* 2010, 58, 1721–1731.
- [6] Tan ZH, Pang BJ, Qin DT. *Mater. Sci. Eng. A*, 2008, 489, 302–309.
- [7] Liu B, Huang WM, Huang L. *Mater. Sci. Eng. A* 2012, 534, 530–535.
- [8] Perng CC, Hwang JR, Doon JL. *Scr. Metall. Mater.* 1993, 29, 311–316.
- [9] Zhu Y, Pang BJ, Shi JY, Wang LW, Gai BZh. *Acta Mater. Compos. Sin.* 2010, 27, 62–67.
- [10] Leduc PR, Bao G. *Int. J. Solids Struct.* 1997, 34, 1563–1581.
- [11] Zhou YX, Xia YM. *Compos. Sci. Technol.* 2000, 60, 403–410.
- [12] Song SG, Shi N, Gray GT. *Metall. Mater. Trans. A* 1996, 27, 3739–3746.